Planetary and Space Science 136 (2017) 34–45

Contents lists available at ScienceDirect

Planetary and Space Science

journal homepage: www.elsevier.com/locate/pss

Magnetic signatures of ion cyclotron waves during Cassini's high-inclination orbits of Saturn

Zachary Meeks*, Sven Simon

School of Earth and Atmospheric Sciences, Georgia Institute of Technology, 311 Ferst Drive, Atlanta, GA 30332-0340, USA

ARTICLE INFO

Keywords:
Ion cyclotron waves
Saturn's magnetosphere
Cassini
Magnetic field

ABSTRACT

Based on magnetic field data from Cassini's high-inclination orbits of Saturn (radius $R_S = 60,268$ km), we analyze the latitudinal distribution of ion cyclotron waves in the giant planet's magnetosphere. Our survey takes into account magnetic field data from all high-inclination orbits between 2004 and 2015. We analyze the dependency of the occurrence rate and amplitude of the ion cyclotron waves on radial distance ρ to Saturn's rotation axis, vertical distance z to Saturn's equatorial plane, and magnetic latitude λ. The occurrence rate of ion cyclotron waves is approximately 100% in Saturn's equatorial plane between the orbits of Enceladus and Dione and decreases to 50% at altitudes of $|z| \approx 0.6R_S$. Ion cyclotron waves were detected up to $|z| = 2.0R_S$. The occurrence rate displays strong, non-monotonic variations with respect to ρ, z, and λ. The vertical amplitude profile of the waves exhibits an M-like pattern with two distinct peaks near $z = \pm 0.3R_S$ and the central minimum at $z = 0$. Compared to earlier observations, we find this M-like structure to be inflated in $\pm z$ direction by a factor of three. The available magnetic field data provides only weak evidence for a local impact of Enceladus and Dione on the ion cyclotron wave field. Using the observed Doppler shift of the ion cyclotron wave frequency during Cassini's high-inclination orbits, we demonstrate the existence of a narrow band of bidirectional wave propagation. This band is centered around Saturn's equatorial plane and possesses a half-width of $|z| = 0.15R_S$, which agrees well with the vertical scale height of Saturn's neutral cloud. To the north of this band, all ion cyclotron waves propagate towards the north ($z > 0$); and to the south, all waves propagate towards the south ($z < 0$). In companion with our previous study (Meeks et al., 2016), this survey provides the complete three-dimensional picture of the ion cyclotron wave field between the orbits of Enceladus and Rhea during the Cassini era.

1. Introduction

The Saturnian system is populated by neutral and charged particles originating from the solar wind and the giant planet's various moons and ionosphere. The main contributor, Enceladus, fills Saturn's magnetosphere with water-group neutrals, which are ejected from the moon's *tiger stripe* features, geysers located near its south pole (e.g., Dougherty et al., 2006; Hansen et al., 2006; Porco et al., 2006; Waite et al., 2006). Some of these neutrals are ionized via charge exchange with the magnetospheric plasma, electron impacts, and solar UV radiation. These newly-generated ions move with Keplerian speed and are then accelerated up to (nearly) corotation with Saturn. This acceleration occurs along cycloidal trajectories due to the $\underline{E} \times \underline{B}$–drift. Because of this motion, the newly-ionized particles form a ring distribution in velocity space, which subsequently thermalizes on time scales of days, thereby releasing the energy surplus in the form of *ion cyclotron waves* (Cowee et al., 2009; Huddleston and Johnstone, 1992). These are left-hand polarized waves with a frequency near the ion gyrofrequency. The amplitude of the ion cyclotron waves can be used to estimate the local ion production rate (Cowee et al., 2009; Huddleston and Johnstone, 1992).

A majority of studies on ion cyclotron waves in Saturn's magnetosphere (e.g., Leisner et al., 2006; Russell et al., 2006; Rodriguez-Martinez et al., 2010)) have focused on the analysis of wave signatures in magnetometer data from Cassini's equatorial orbits. In this context, an equatorial orbit is defined as any orbit where the inclination of Cassini's trajectory relative to Saturn's equatorial plane is less than 5°. Recently, Meeks et al. (2016) searched all of Cassini's equatorial orbital segments (4.4 years of data in total) for ion cyclotron waves. This study demonstrated that the occurrence rate of ion cyclotron waves, R_{ICW}, displays a Fermi-Dirac-like profile with respect to L-Shell, with $R_{ICW} \approx 100\%$ between $L = 3.9$ and $L = 5.5$. Also, this survey found no ion cyclotron waves occurring past $L = 8.1$. Along with the occurrence rate, Meeks et al. (2016) showed that the amplitude of the ion cyclotron

---

* Corresponding author.
E-mail address: zachary.meeks@gatech.edu (Z. Meeks).

http://dx.doi.org/10.1016/j.pss.2016.12.006
Received 20 September 2016; Received in revised form 8 December 2016; Accepted 21 December 2016

waves remains approximately constant between the orbits of Enceladus (at $L=3.9$) and Dione (at $L=6.3$). During Cassini's equatorial orbits, neither the occurrence rate nor the amplitude displayed a dependency on Local Time or azimuthal distance from Saturn's icy moons Enceladus, Dione, and Rhea.

Unlike the previously mentioned studies, Leisner et al. (2011) analyzed ion cyclotron waves from four high-inclination orbits (i.e., inclination greater than 5° relative to Saturn's equatorial plane) between October 2006 and December 2006. These authors demonstrated that a Doppler shift is visible in the magnetic power spectral density of the waves. This shift causes the measured frequency of the ion cyclotron waves to be higher than the local water ion gyrofrequency $\Omega_{H_2O^+}$ when Cassini moves anti-parallel to the direction of wave propagation and lower then $\Omega_{H_2O^+}$ when Cassini moves parallel to the waves. This effect did not play a role in our previous study of equatorial orbits because Cassini's trajectory was very nearly perpendicular to the wave propagation direction (Meeks et al., 2016).

By combining the Doppler shift of the wave frequencies with the direction of Cassini's motion, Leisner et al. (2011) were able to identify a narrow band of thickness $\pm 0.1R_S$ (Radius of Saturn: $R_S = 60,268$ km) around Saturn's equatorial plane where the ion cyclotron waves propagated both northward and southward. In such a region where waves propagate in both directions, the waves will generate two distinct peaks in the power spectrum, which are displaced symmetrically with respect to the local water gyrofrequency. Leisner et al. (2011) interpreted this layer as a wave generation region. To the north of this equatorial wave generation layer, the ion cyclotron waves were found to propagate northward; and to the south, they were found to propagate southward. Hence, the waves propagate *away* from the equatorial plane in both hemispheres. Leisner et al. (2011) also found that the amplitude of the observed ion cyclotron waves initially increased with distance z to Saturn's equatorial plane, reaching its maximum near $z = \pm 0.2R_S$, and then faded before $z = \pm 0.4R_S$.

As demonstrated by Meeks et al. (2016), the conclusions drawn by preceding studies for the *equatorial* orbital segments, which were based on between 1 day and 457 days of data, often did not hold true when compared against the results of the comprehensive 4.4-year analysis. In the present study, we therefore search all segments of Cassini's *high-inclination* orbits which fall within $L=3.8$ and $L=8.1$ (i.e., the region identified as containing ion cyclotron waves by Meeks et al. (2016)) for signatures of ion cyclotron waves. Our study therefore greatly amplifies the initial survey of the high-inclination orbits by Leisner et al. (2011), which was based on only four orbital segments.

As shown in Fig. 1, this survey will consider the magnetic field data from April 2005 to August 2005, July 2006 to June 2007, November 2007 to October 2009, and May 2012 to June 2015 (5.3 years in total). This dataset includes 54 orbital segments which intersect the equatorial plane of Saturn within or near the ring of high R_{ICW} (i.e., $3.8 \leq L \leq 5.5$) identified by Meeks et al. (2016). In this way, we will expand the two-dimensional characterization from our previous study to a comprehensive three-dimensional picture of the ion cyclotron wave field in Saturn's magnetosphere. Also, because Cassini's “Grand Finale” orbits will intersect the equatorial plane well inside of the orbit of Enceladus, this study presents the complete picture of ion cyclotron waves during the high-inclination orbits between Enceladus and Rhea.

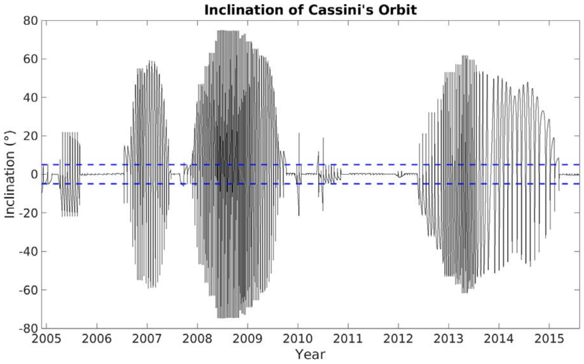

Fig. 1. Inclination of Cassini's trajectory with respect to Saturn's equatorial plane between November 2004 and August 2015. The orbits that pass the blue dashed lines (located at ±5° latitude) are classified as high-inclination, while the other orbits are classified as low-inclination. The magnetic field data from the low-inclination orbits have already been searched for ion cyclotron waves by Meeks et al. (2016). The inclination of the orbits considered in the present study ranges from 10° to 75°. (For interpretation of the references to color in this figure legend, the reader is referred to the web version of this article.)

Following the style of Meeks et al. (2016), the structure of this study is as follows: in Section 2, we discuss the process used to identify ion cyclotron waves in the magnetic field data. In Section 3, we present a search of the entire magnetic field dataset for ion cyclotron waves and discuss the potential dependence of their *occurrence* on radial distance to Saturn's rotation axis, vertical distance to Saturn's equatorial plane, and magnetic latitude λ. In Section 4, we present a study of the ion cyclotron wave *amplitudes* for the entire trajectory segment. In Section 5, we present a study of the propagation direction of ion cyclotron waves. Utilizing the Doppler shift, we identify the vertical extent of the wave generation region (characterized by bidirectional propagation). We also characterize the propagation directions of waves outside of this region. Finally, in Section 6, we summarize our major results.

2. Identification of ion cyclotron waves

The Cartesian coordinate system (x, y, z) used in this study is centered at Saturn. The x-axis is directed towards 00:00 Local Time (LT, midnight), whereas the y-axis is directed towards 06:00 Local Time (dawn). The z-axis is parallel to Saturn's rotation axis. In this context, the parameter $\rho = \sqrt{x^2 + y^2}$ denotes the radial distance to Saturn's rotation axis. In the equatorial plane, ρ is equivalent to the L-Shell parameter. The magnetometer data are displayed in spherical coordinates (B_r, B_Θ, B_ϕ) with B_r directed away from Saturn, B_Θ directed parallel to Saturn's background magnetic field, and B_ϕ directed in the azimuthal direction (i.e., the direction of corotation).

We divide the magnetometer data from the entire 5.3 year dataset into intervals of height $\Delta z_{int} = 0.02R_S$. The search for ion cyclotron waves was constrained to orbital segments for which Cassini's position was within a hollow cylinder with inner radius $\rho = 3.8R_S$, outer radius $\rho = 8.1R_S$, and height between $z = -5R_S$ and $z = 5R_S$. This analysis region contains 54 orbital segments. Almost all of them intersect the equatorial plane within the “ring” of $R_{ICW} \approx 1$ between $L=3.8$ and $L=5.5$ that was identified by Meeks et al. (2016). These intersections (denoted by the crosses in Fig. 2) have coverage across most Local Times and ρ values between the orbits of Enceladus and Dione, although the sampling density in radial (ρ) and azimuthal (Local Time) directions is much lower than in our preceding study of the equatorial orbits. For some Local Time sectors (e.g., 05:00 LT to 07:00 LT and 13:00 LT to 18:00 LT), the intersections cluster near the orbits of Enceladus and Dione (see Fig. 2), which leaves gaps in our radial data coverage between these two moons. Besides, a few segments (04:00 LT to 05:00 LT and 13:00 LT to 15:00 LT) have sparse coverage in both Local Time and radial direction (ρ) or are not even covered at all.

For this study, we use magnetometer (Dougherty et al. (2004)) data with 1-second resolution. To isolate the waves “riding” on the background magnetospheric field, we detrend the data by subtracting the average magnetic field strength from a 20-min window centered on each point in the Δz_{int}-intervals. In analogy to Meeks et al. (2016), we then calculate the power spectrum of all magnetic field components, along with the compressional and transverse power spectra, for each Δz_{int}-interval.

Unlike Meeks et al. (2016), the identification of ion cyclotron waves is now based on a combination of a *global* and a set of *local* criteria: the